Photofission of ^{238}U with 100, 500, and 1000 MeV/u ^{208}Pb ions

W. Brüchle, H. Folger, E. Jäger, T. Krogulski, S. Polikanov, M. Schädel, E. Schimpf, G. Wirth
GSI, Darmstadt
Th. Aumann, J.V. Kratz, E. Stiel, N. Trautmann
Institut für Kernchemie, Universität Mainz

We have performed fission studies of ^{238}U in the reaction with 100, 500, and 1000 MeV/nucleon ^{208}Pb ions by detecting in coincidence two fragments emitted from a thin U target[1]. The experiments were carried out at SIS with a setup consisting of six low-pressure multiwire proportional counters mounted in USCHI[2]. To detect the fission fragments emitted as a result of the prompt fission, the counters were arranged in such a geometry that two of them (the start counters) produced the zero-time signals. The other four counters (the stop counters) produced the signals required to measure the time of flight, and, apart from that, they measured the ionization produced by the fragments. As a result, we have obtained data on velocities and folding angles of the fission fragments emitted in the ^{208}Pb+^{238}U reaction.

In our analysis of the experimental data we employed the fact that the momentum-transfer distribntions as well as the mass distributions of fission fragments are different in nuclear fission and photofission, which occurs as a result of the giant-dipole-resonance excitation. These differences enabled us to estimate the probability of photofission in the ^{208}Pb+^{238}U reaction. This probability was determined from a comparison of the experimental velocity and angle distributions with those obtained in Monte Carlo simulations.

In a Monte Carlo simulation of photofission, the parallel-momentum transfer to the nucleus was taken as zero, and the perpendicular-momentum-transfer distribution was calculated according to Ref. 3. The kinetic energy of the fragments and the mass spectra for photofission were taken from Refs. 4 and 5 respectively, so that there were no free parameters used in our analysis of photofission.

To simulate the distribntions for nuclear fission we have chosen the parallel-momentum transfer distribution in the form $F(p_{||}) = (p_{||}/p_{||0})\exp(-(p_{||}/p_{||0}))$, where $p_{||0}$ is a free parameter. The perpendicular-momentum transfer distribution was chosen in the form of Gaussian centered at the average perpendicular-momentum transfer $p_\perp$ with a dispersion $dp_\perp$. The dispersion of of the symmetric fragment-mass distribution was a free parameter., It was shown that varying it from 12 u to 18 u we do not significantly change the results of analysis. As the influence of $dp_\perp$ is also small the folding- and azimuthal-angle distributions as well as the velocity distributions are only sensitive to the two parameters $p_{||0}$ and $p_\perp$.

The resulting distributions were the sums of the distributions for nuclear fission and photofission, with the fraction of photofission W ($W = \sigma_{\gamma f}/(\sigma_{\gamma f}+\sigma_{nucl f})$) as a free parameter. The simulated velocity, and folding- and azimuthal-angle distributions were fitted to the measured distributions. The values of W corresponding to the minimum χ^2 value are given in Table I for 100, 500, 1000 MeV/u ^{208}Pb.

Table I. The fraction of photofission W in the reaction ^{208}Pb+^{238}U.

Energy MeV/u	100	500	1000
$\frac{\sigma_{\gamma f}}{\sigma_{\gamma f}+\sigma_{nucl f}}$	0.19 ±0.06	0.45 ±0.08	0.61 ±0.03

As one example, we show in Fig.1 the measured and calculated folding-angle distributions. The shape of these distributions changes with the incident-ion energy. This is because the momentum transfer as well as the contributions of photofission depend on the Pb-nucleus energy.

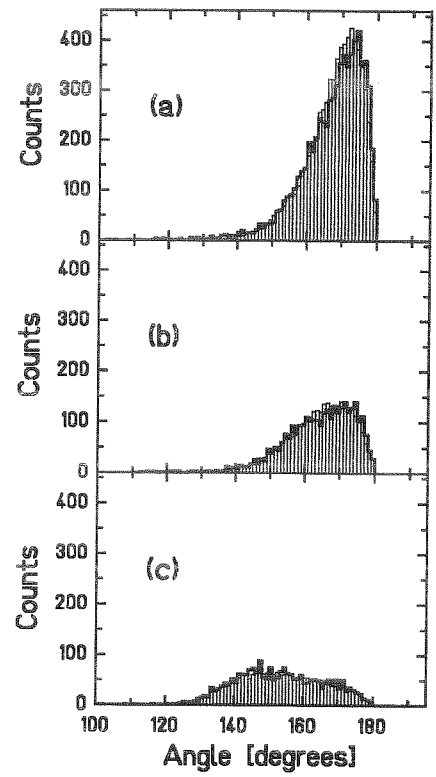

FIG. 1. The folding-angle distribution for the fission fragments from the ^{208}Pb+^{238}U reaction: (a) - 1000 MeV/nucleon, (b) - 500 MeV/nucleon, (c) - 100 MeV/ nucleon. The solid lines are the experimental results, and the hatched distributions are the results of calculations corresponding to W in Table I.

The results of our analysis do not exclude that some fraction of asymmetric fission, small at energies 500 and 1000 MeV/u, comes from the low energy fission of ^{238}U excited in nuclear interactions.

REFERENCES

[1] T.Krogulski et al. Scientific Report, GSI 93-1 (1993) p. 64
[2] E.Stiel et al. Scientific Report, GSI 91-1 (1991) p. 323
[3] J.D.Jackson, Classical Electrodynamics (Wiley, New York, 1975), p. 520
[4] V.E.Viola, Nucl.Data, Sect. A1, 391(1966)
[5] E.Jacobs et al., Phys. Rev. C19, 422(1979)

Solvent induced track sensitization

P. Apel[♣], N. Angert[◇], W. Brüchle[◇], H. Fuess[*], H. Hermann[◇], U. Kampschulte[◇], P. Klein[◇], L.I. Kravets[♣], Yu.Ts. Oganessian[♣], G. Remmert[☆], R. Spohr[◇], T. Steckenreiter[*], C. Trautmann[◇], J. Vetter[◇]

[♣]JINR Dubna, [◇]GSI Darmstadt, [◇]Hoechst AG Frankfurt, [☆]Univ. Frankfurt, [*]Tech. Hochschule Darmstadt

Introduction

A necessary condition for particle track etching in polymers is the selective removal of molecular fragments formed along the ion path. Solvent induced track sensitization [1] removes oligomers from the track core [2] and generates electrolytically conducting paths [3] resembling very fine pores.

Experimental

Oligomer extraction from 19 µm polyethylene terephthalate (PET) by dimethylformamide (DMF) irradiated by heavy ions was investigated by gel permeation chromatography (GPC) and UV spectroscopy. Sensitization dynamics were studied in a conductivity cell using DMF diluted by 10% water with small amounts of potassium halides. Degree of crystallinity was studied by differential scanning-calorimetry (DSC).

Results and discussion

After irradiation a distinct band of radiolysis products with molecular masses between 500 and 2000 appeared in the GPC spectrum (figure 1). The cyclic trimer was identified as dominant extracted diffusing species. Extraction dynamics was modelized by a rapid ($\tau \approx 2$ min) and a slow ($\tau \approx 100$ min) diffusion process attributed to the latent ion tracks and to the virgin material, respectively. Thereby latent tracks (zones with reduced density [4]) act as drainage pipes for the extraction of oligomers from the polymer matrix.

Experiments with the electrolytic conductivity cell confirmed that the sensitization process is governed by DMF diffusion, with an activation energy of 88.2 kJ/mol. The time required for observation of conductivity through tracks depends strongly on the halide anion radius in the electrolyte (90%DMF+10%H_2O+0.1m potassium halides) (figure 2).

The crystallinity of virgin material of 48.2% was decreased after ion irradiation (8.5 10^{10} U ions / cm^2) to 47.4%. DMF treatment (1.5h, 60 °C) leads to further amorphization by 6%.

Conclusion

Extraction dynamics can be explained by the drainage model. The cyclic trimer predominates among the extracted molecules. Further investigations should be focused on a detailed analysis of the extracted molecules.

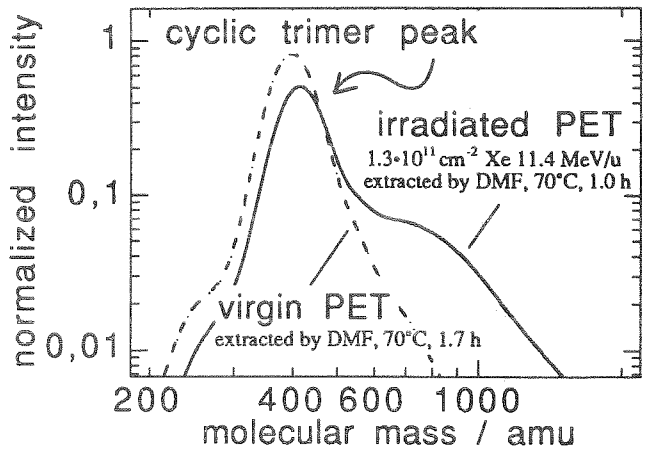

Figure 1. GPC spectra of extracts from virgin and irradiated PET. Irradiation creates in the polymer a new fraction of easily extractable oligomers.

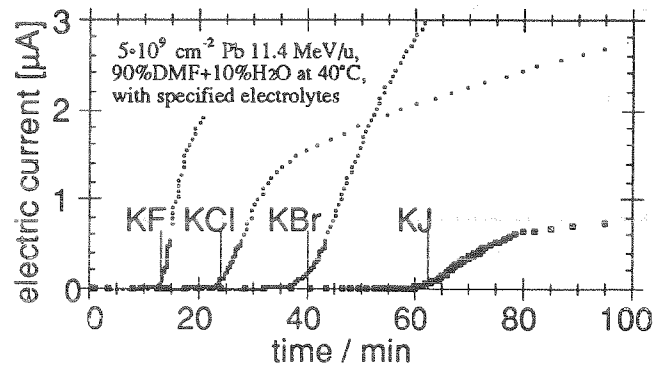

Figure 2. Electrolytic conductivity of ion tracks in DMF depends systematically on effective electrolytic ion radius, the smallest ion (F^-) penetrating earliest.

[1] H. B. Lueck; Nucl. Tracks Radiat. Meas., 19, (nos. 1-4), pp. 189-195, (1991).

[2] P. Apel, N. Angert, W. Brüchle, H. Herrmann, U. Kampschulte, P. Klein, L.I. Kravets, Yu. Ts. Oganessian, G. Remmert, R. Spohr, T. Steckenreiter, C. Trautmann, J. Vetter; NIM B, (1993), to be published.

[3] Th. Steckenreiter, Diplomarbeit TH Darmstadt and GSI Darmstadt, (1994).

[4] K. Schaupert, D. Albrecht, P. Armbruster, R. Spohr; Appl. Phys. A 44, pp. 347-352 (1987).

Enhancement of Transport Critical Current Density in Bi-2212 Superconducting Thin Films by Heavy-Ion Irradiation[B]

[a,b]J. Wiesner, [b]G. Wirth, [a]H. Fueß, [c]P. Wagner, [c]F. Hillmer, [c]H. Adrian, [b]E. Jäger, [b]E. Schimpf
[a]Fachbereich Materialwissenschaft TH Darmstadt, [b]GSI Darmstadt, [c]Institut für Festkörperphysik TH Darmstadt

The critical current densities of high temperature superconductors are still too small for a broad range of technological applications. The main material-intrinsic current limiting process is dissipation due to the motion of magnetic flux lines penetrating a superconductor. Lattice defects - especially those which are produced by heavy-ion irradiation - can hinder this motion by local pinning [1,2].

The low temperature irradiation facility at the heavy-ion accelerator UNILAC was used for the investigation of high-T_c superconducting samples. It enables in-situ measurements of the resistive transition R(T) and transport critical current densities J_{ct} in thin film microbridges using the standard four point method in magnetic fields up to 1.1 T. This allows us to study the ion dose dependent change of J_{ct} and R(T) using a single sample. Thus we avoid uncertainties which arise when data of different samples are compared. J_{ct}-measurements at higher magnetic fields and magnetization measurements of heavy ion irradiated samples were performed off-line.

Columnar defects consisting of amorphous tubes with a typical diameter of 10nm were created in epitaxial Bi-2212 films with a thickness of about 300nm[3] by irradiation with 1.16 GeV ^{197}Au- and 1.4 GeV ^{238}U-ions. The defects were characterized by HRTEM [4].

Fig. 1 shows J_{ct} as a function of magnetic field for a Bi-2212 thin film irradiated with 1.4 GeV ^{238}U-ions to different doses. In the range of 10^{10} - 10^{11} ions/cm^2 we observed a field dependent increase of J_{ct} with the applied dose. Depending on ion dose and magnetic field we found enhancement factors of up to 150 (Fig. 3). The decrease of J_{ct} at low magnetic fields and high ion doses ($4\text{-}6 \cdot 10^{10}$ ions/cm^2) can be related to the degradation of T_c.

Considering the statistical distribution of the tracks[4] it is very likely that not each vortex of a matching field B_Φ, where the number of vortices equals the number of defects, will be pinned by a track. Therefore a maximum pinning effect should be expected for $B_\Phi > B$. Differing from that we found that the field B_{max} at which the maximum of the J_{ct}-enhancement is found shifts with increasing ion dose with respect to B_Φ. A continuous development from $B_{max} > B_\Phi$ to $B_{max} < B_\Phi$ is observed (Fig. 2,3).

Heating the samples to room temperature after irradiation led to a further increase of J_{ct} by factors of 1.5 to 2 for different temperatures from 40K to 70K. Fig. 4 shows the corresponding data at 57K. We assume that this effect is connected with diffusion of oxygen and therefore a partly recovery of small damaged regions outside the tracks.

This work is financially supported by the Bundesministerium für Forschung und Technologie and the Hoechst AG, Frankfurt.

REFERENCES

1) W. Gerhäuser, H.-W. Neumüller, W. Schmidt, G. Ries, O. Eibl, G. Saemann-Ischenko, S. Klaumünzer, Physica C 185-189, p. 2339 (1991)

2) D. Bourgault, S. Bouffard, M. Toulemonde, D. Groult, J. Provost, F. Studer, N.Nguyen, B. Raveau, Phys. Rev. B39 (10), p. 6549 (1.4.1989)

3) P. Wagner, H. Adrian, C. Tomé-Rosa, Physica C 195 (1992), p. 258

4) H.W. Zandbergen, C. Traeholt, J.-G. Wen, G. Wirth, E. Jaeger, E. Schimpf, J. Wiesner, H. Fueß, in this annual report

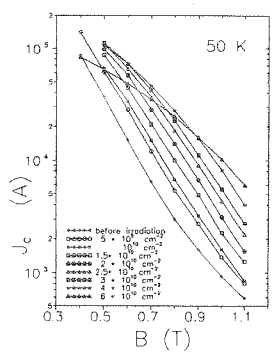

Fig. 1: *J_{ct} as a function of the magnetic field B at 50K of a film irradiated with ^{238}U-ions.*

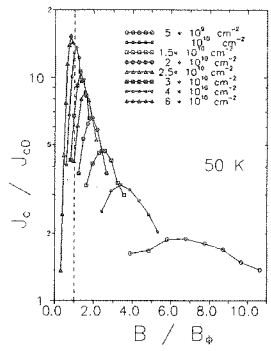

Fig. 2: *J_{ct}-enhancement as a function of B normalized to B_Φ at 50K. Same film as in Fig. 1.*

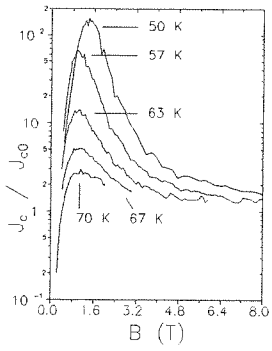

Fig. 3: *J_{ct}-enhancement of a film irradiated with ^{238}U-ions to a dose of 10^{11} ions/cm^2 (B_Φ = 2T).*

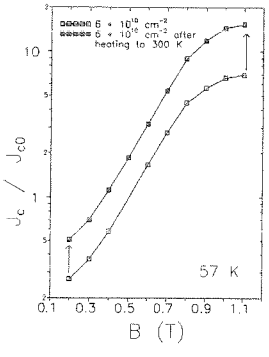

Fig. 4: *J_{ct}-enhancement of a film irradiated with $6 \cdot 10^{10}$/cm^2 ^{197}Au-ions before and after heating to 300K.*

HRTEM-Characterization of Heavy-Ion-Induced Defects in Bi-2212 Superconducting Thin Films[B]

[a]H.W. Zandbergen, [a]C. Traeholt, [c]J.-G. Wen, [b]G. Wirth, [b]E. Jäger, [b]E. Schimpf, [b,c]J. Wiesner, [c]H. Fueß
[a]NCHREM Laboratory for Materials Science Delft University of Technology, [b]GSI Darmstadt,
[c]Fachbereich Materialwissenschaft TH Darmstadt

We have investigated the defect creation by heavy-ion irradiation in high temperature superconductors (HTS) by high resolution transmission electron microscopy (HRTEM) and in-situ measurements of the critical current density J_{ct}. Defects in the otherwise crystalline HTS - whether they are due to preparation or introduced artificially - act as pinning centers for magnetic flux lines penetrating a superconductor. Thus they influence the loss-free current a superconductor can carry which is an important property for technological applications.

Epitaxial Bi-2212 films with a thickness of about 300nm[1] were irradiated with ^{40}Ca- (Energy = 200 MeV), ^{197}Au- (1.16 GeV) and ^{238}U-ions (1.4 GeV). According to calculations with the TRIM-code these ions pass through the superconducting thin film with an electronic energy loss ($dE/dx_{el.}$) of 660, 3870 and 4510 eV/Å respectively.

The type of crystal defects created by heavy-ion irradiation strongly depends on the electronic energy loss $dE/dx_{el.}$ of the ions and on the material itself. With increasing $dE/dx_{el.}$ a transition from randomly distributed displacement cascades to amorphous columns along the ion path is expected. Latent tracks in Bi-2212 were reported for a $dE/dx_{el.}$ - value of 2500 eV/Å [2].

HRTEM was used to characterize the defects produced by ^{238}U- and ^{40}Ca-ions in Bi-2212 thin films. In the Ca-irradiated sample no latent tracks were found in agreement with the low electronic energy loss given above. On the other hand each ^{238}U-ion did produce a well defined latent columnar track as expected.

The top view of an ^{238}U-ion-irradiated film (Fig. 1) shows the statistical distribution of tracks with a typical diameter of 10nm. Each track - one viewed in high magnification in Fig. 2 - consists of totally amorphized material. It seems to be interrupted for a short distance in the substrate at the interface but it is yet not clear whether this is due to the sample preparation for TEM-analysis or if it indicates a recrystallisation process. Images of a larger sample area show this interruption for all ion tracks although they reach deep into the substrate as it is expected from the TRIM-calculations. The sometimes smeared transition between amorphous and crystalline material is caused by the finite thickness of the HRTEM-sample. It leads to a superposition of the contrasts of crystalline and amorphous material at the borders of the cylindrical track. At higher magnification - resolving single atoms - a sharp transition between amorphized and crystalline material at the track border was observed (Fig. 3). Apart from that observation it seems very likely that there are further defects on an atomar scale (e.g. Frenkel-pairs) outside the amorphous core of the columnar track. Such additional defects might present an explanation for the annealing effect which is described elsewhere [3].

The great difference in defect production between ions with low and high $dE/dx_{el.}$ should be reflected in J_{ct}-measurements since the pinning strength depends strongly on the type and extent of the defects.

Therefore in-situ-measurements of J_{ct} were performed at our low temperature irradiation facility [3]. ^{40}Ca-ions (200 MeV) were applied to a structured Bi-2212 film which didn't produce columnar tracks but scattered localized defects like displacement cascades. At a dose of $5 \cdot 10^{11}$ ions/cm² the maximum enhancement at 50 K only by a factor of 3 was reached. A further irradiation of the same sample with ^{197}Au-ions (1.16 GeV) led to a maximum J_{ct}-enhancement by a factor of 22 (7 times the maximum of the Ca-irradiation) using a dose of $7 \cdot 10^{10}$ ions/cm². This clearly shows that columnar tracks are the most effective pinning centers (Fig. 4).

This work is financially supported by the Bundesministerium für Forschung und Technologie and the Hoechst AG, Frankfurt.

REFERENCES

1) P. Wagner, H. Adrian, C. Tomé-Rosa, Physica C 195 (1992), p. 258
2) W. Gerhäuser, H.-W. Neumüller, W. Schmidt, G. Ries, O. Eibl, G. Saemann-Ischenko, S. Klaumünzer, Physica C 185-189, p. 2339 (1991)
3) J. Wiesner, G. Wirth, E. Jaeger, E. Schimpf, H. Fueß, P. Wagner, F. Hillmer, H. Adrian, in this annual report

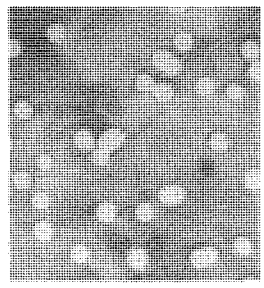

Fig.1: *Top view of Bi-2212 film irradiated with 10^{11} ^{238}U-ions/cm². Track-Ø = 10nm.*

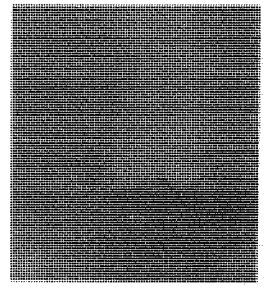

Fig. 2: *Cross-section of an ion track in the same sample at the interface between film (top) and substrate.*

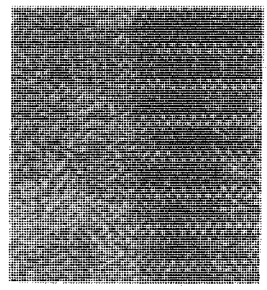

Fig. 3: *High resolution cross-section of the boundary between an ion track and the surrounding Bi-2212 material.*

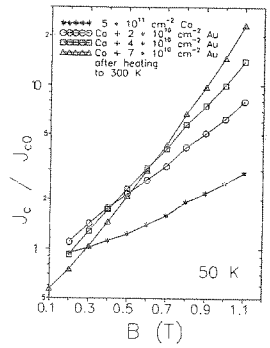

Fig. 4: *Comparison of J_{ct} -enhancement after irradiation with ^{40}Ca- and ^{197}Au-ions.*

Twinning of YBa2Cu3O7 thin films on different substrates and modification by heavy-ion irradiation[B]

[a]T. Steinborn, [a]G. Miehe, [a,b]J. Wiesner, [a]H. Fueß, [b]G. Wirth
[a]Strukturforschung, Fachbereich Materialwissenschaft TH Darmstadt, [b]GSI Darmstadt

The crystal structure of $YBa_2Cu_3O_{7-\delta}$ (YBCO) is tetragonal for δ=1 and orthorhombic for δ=0. For δ>0.6 no superconductivity is observed. Usually the orthorhombic phase of YBCO (δ=0) is twinned. It is expected that the twinning geometry influences the electric and magnetic properties of the films: For twinned single crystals Durán et al.[1] observed a preferential magnetic flux penetration along the twin boundaries.

In order to interpret the transport properties such as the critical current density the twin structure in the a-b plane is analysed. The type of twinning is correlated with the structure of the substrate [2].

Up to now irradiation experiments with high-T_c-superconductors [3][4] were mainly concerned with the development of T_c, j_c and latent track formation. Apart from the broadening of 00l-peaks, no detailed results of X-ray-diffraction experiments have been reported.

x-ray data for the samples were collected at a STOE four-circle diffractometer with graphite monochromatized Co K_α radiation, a divergence of 0.3° and synchrotron radiation (HASYLAB λ=0.56 and 0.71Å). The splittig of YBCO reflections is a result of the twinning of YBCO with $(1\bar{1}0)$ and (110) as planes of intergrowth.

During irradiation the <hh0> alignment (Fig.1a) gradually transforms to an <100> alignment (Fig.1d). Obviously fractions of the film are enabled to reorient independently. The complete transformation is connected with a rotation of ±0.45° around c.

This "detwinning" after irradiation was observed for YBCO films on $NdGaO_3$ and MgO as well. For YBCO films on different substrates varied the threshold dose for the realignment. Besides 1.2GeV ^{209}Bi ions 1.4GeV ^{238}U and 1.16 GeV ^{197}Au ions were used.

In $SrTiO_3$ and YBCO, 1.2GeV ^{209}Bi ions have a penetration depth of 40 and 32µm, respectively. Hence they penetrate the film completely and are stopped in the substrate. Let the dose be D and the "average distance" $\delta=D^{-1/2}$. It is easy to show that the true mean distance for the n nearest neighboured impacts is $2/3\cdot\delta\cdot(n/\pi)^{1/2}$ which is 0.376δ for n=1 and e.g. 0.752δ for n=4. The modelling of randomly distributed impacts shows that the distribution function has a considerable halfwidth which is about 0.6δ for n=1 and 0.5δ for n=4.

For a dose $D=5\cdot10^{11}cm^{-2}$ δ is 140Å. TEM observations revealed the diameter of the impact channels to be in the order of 70 to 100Å ([5] and Zandbergen, priv. comm.), the ratio (volume of tracks)/(volume of the layer) ranges from 0.2 to 0.4. In fact the amorphized volume is smaller due to overlapping of channels, but the order of magnitude is still some 10%.

For $D=5\cdot10^{11}cm^{-2}$ the state of the film begins to approach the model of an archipel of crystalline islands of linear dimensions in the order of 100Å - many of them connected with bridges - in a sea of amorphous material. It can be assumed that in the unirradiated film the width of a twin lamella is large compared with 100Å (500Å are reported in [5]). Then the islands containing $(110-\bar{1}10)$ wall junctions are a minority fraction. For the others the <100>alignment becomes favourable since strain due to the misfit is relaxed as soon as it approaches the nearby shore of the island. The intermediate states of the reorientation (Fig.1b,c) represent an equilibrium between the energy minimum for the undestroyed layer which is preserved and transferred by the bridges between the islands and the minimum for the isolated islands which becomes predominant as the bridges are destroyed.

References

[1] C. A. Durán, P.L. Gammel, R. Wolfe, V. J. Fratello, D.J. Bishop, J. P. Rice, D. M. Ginsberg: Nature **357**, 474 (1992)

[2]T. Steinborn; G. Miehe; J. Wiesner; E. Brecht; H. Fuess; G. Wirth; B. Schulte; M. Speckmann; H. Adrian; M. Maul: Physica C, (in print)

[3] B. Roas, B. Hensel, S. Henke, S. Klaumünzer, B. Kabius, W. Watanabe, G. Saemann-Ischenko, L. Schultz, K. Urban: Europhys. Lett. **11** (7), 669 (1990)

[4] F. Rullier-Albenque, A. Legris, S. Bouffard, E. Paumier, P. Lejay: Physica C **175**, 111 (1991)

[5] H. Watanabe, B. Kabius, K. Urban, B. Roas, S. Klaumünzer, G. Saemann-Ischenko: Physica C **179**, 75 (1991)

Fig.1: YBCO on $SrTiO_3$, splitting of the 302 reflection after irradiation with 1.2GeV ^{209}Bi ions to increasing doses:
a) unirradiated, b) $10^{10}/cm^2$, c) $10^{11}/cm^2$, d) $5\cdot10^{11}/cm^2$

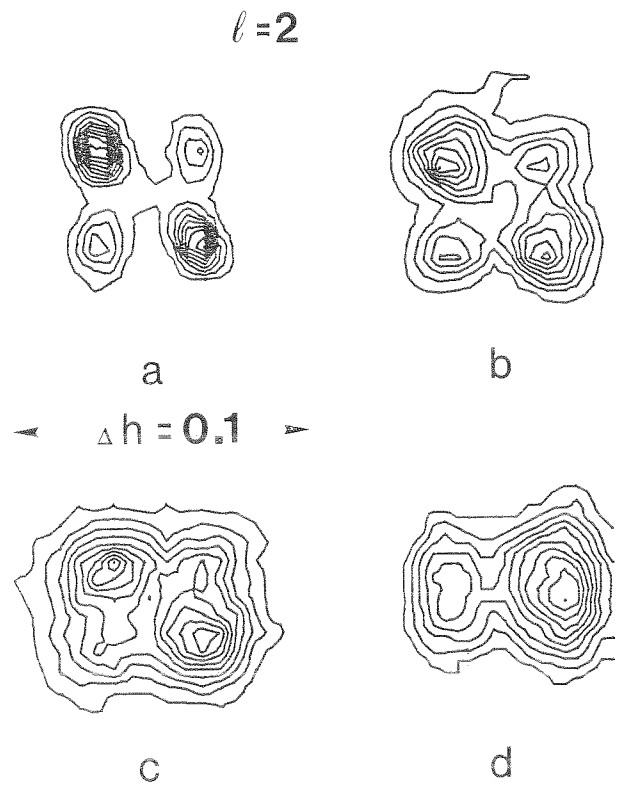

Vortex pinning in ion-irradiated $NbSe_2$ studied by scanning tunneling microscopy

S.Behler, S.H.Pan, P.Jess, A.Baratoff, H.-J.Güntherodt
Institut für Physik, Universität Basel

F.Lévy
Institut de Physique Appliquée, Ecole Polytechnique Fédérale de Lausanne

G.Wirth, J.Wiesner
GSI, Darmstadt

In the Shubnikov phase of a type-II superconductor lattice defects of various types can hinder the motion of vortices by local pinning and enable the superconductor to carry large lossless currents. Columnar line defects can be produced by swift heavy ions and these amorphous tubes act as very effective pinning centers. The measurement of the critcal current density of a sample after the introduction of defects by heavy ion irridiation gives kind of macroscopic data averaging over many magnetic flux lines and defects present in one sample. A more microscopic view deals with the spatial arrangement of the vortices and a possible distortion of the vortex lattice by pinning centers. For the first time the interaction of vortices with individual defects has been visualized by means of low temperature scanning tunneling microscopy STM [1]. This method can yield simultaneous images of the surface topography and of the vortices with high resolution. The vortex arrangement observed at a temperature of 3K can directly be related to columnar line defects introduced by Au-ions into a $NbSe_2$ crystal.

The vortex lattice is imaged by scanning the irradiated sample in the STM constant current mode at a bias voltage of 0.5 mV. Due to its reduced tunnel conductance at a bias voltage within the superconducting gap (1 mV), the superconducting matrix appears slightly lower than the vortices. As a consequence the STM image contains superimposed topographic and spectroscopic information. Images taken at a bias of 5.0 mV display the surface topography alone.

Non-irradiated $NbSe_2$ crystals exhibit an essentially triangular vortex lattice with a spacing of $a_{VL} = 489\ \text{Å}/B^{1/2}$, where B is the external magnetic field in Tesla. In contrast, the irradiated $NbSe_2$ crystal shows a different behavior.

Fig. 1a shows a 2 x 2 μm^2 STM image of the vortex lattice at 500mT. It is strongly distorted as can easily be seen by viewing adjacent rows of vortices. The apparent distortion of the vortex arrangement is attributed to pinning by columnar defects, which are hardly visible in the figure due to their small size. In order to relate the vortex arrangement to the defects, the center part of Fig. 1a is imaged with higher resolution. Fig. 1b is an 0.8 x 0.8 μm^2 image which displays the surface topography. Five defects with an inner diameter of 10 nm are clearly visible (see inset). They can be associated with columnar defects generated by heavy ion irradiation. The STM images in Fig. 1c,d display vortex arrangements on the same surface area as Fig. 1b observed at different external magnetic fields. White circles indicate the location of the defects. Fig. 1c is taken at 100 mT. All five defects pin a vortex and induce irregularities and deformations in the vortex arrangement. This can also be seen in the center part of Fig. 1a, where the location of the five defects are marked by circles. The radiation-induced defects can thus clearly be identified as efficient pinning sites. Fig. 1d shows the vortex arrangement at 30 mT. Note that at this low vortex density not all of the defects pin a vortex. A weak repulsion between vortices is likely preventing the more inhomogeneous arrangement which would result if each vortex "condensed" on a defect.

REFERENCES

[1] S.Behler, S.H.Pan, P.Jess, A.Baratoff, H.J.Güntherodt, F.Lévy G.Wirth, J.Wiesner
Phys. Rev. Lett., submitted

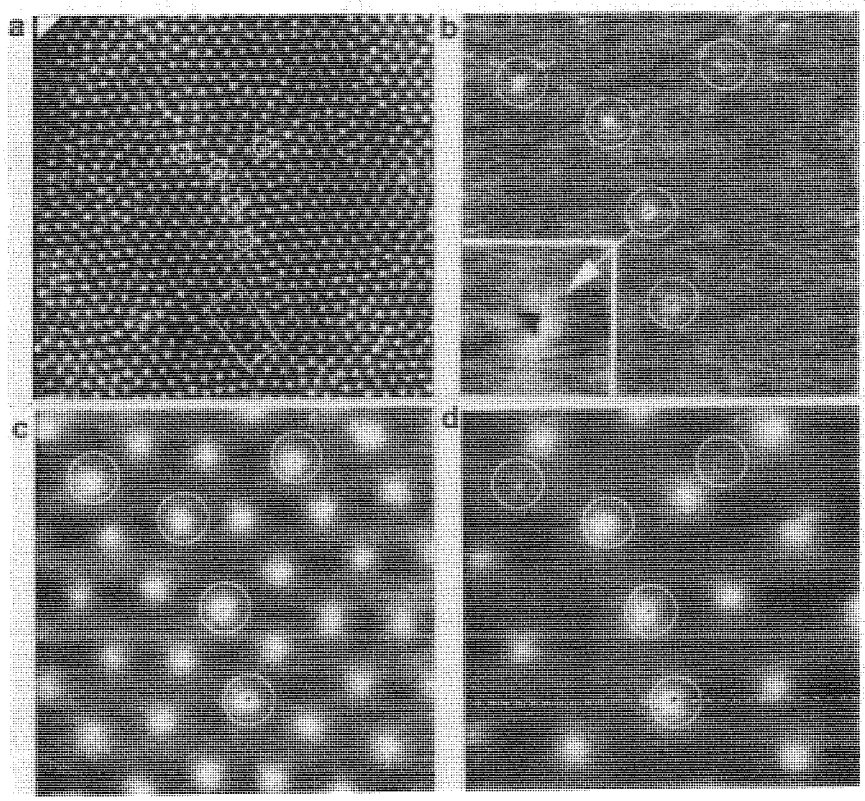

Fig 1: (a) 2x2 μm^2 STM image of the distorted vortex lattice in ion-irradiated $NbSe_2$ at 500mT and 3K. The circles indicate defect locations extracted from (b). (b) 0.8x0.8 μm^2 STM image of the surface topography showing defects created by ion irradiation - inset 50x50 nm^2 image of one defect. (c,d) images of vortex arrangements within the same area as (b) acquired at 100 and 30 mT. The radiation defects are marked by white circles.

Effects of Columnar Defects on the Critical Current Density in $(Bi,Pb)_2Sr_2Ca_2Cu_3O_{10+\delta}$ Silver Sheathed Tapes[B]

P.Kummeth [1,2], C.Struller [2], H.-W.Neumüller [1], G.Ries [1], M.Kraus [2], G.Wirth [3], J.Wiesner [3], O.Eibl [4] and G.Saemann-Ischenko [4]

[1] Siemens AG, Research Laboratories, Erlangen
[2] Physikalisches Institut, Universität Erlangen-Nürnberg
[3] GSI, Darmstadt
[4] Siemens AG, Research Laboratories, München

Among all the presently known techniques to produce high temperature superconductor (HTSC) wires the powder in tube technique based on Bi-compounds is the most promising one. For application of HTSC in power engineering it is necessary to reach critical current densities j_c above 10^5 A/cm^2 in the superconductor. The clear influence of thermal activated depinning in BSCCO-superconductors requires the search for further j_c-enhancement. A reliable method to check possible j_c - improvements in superconductors is based on introducing the most effective type of defects, columnar amorphous tracks, by heavy ion irradiation. The investigations cover both transport and magnetization measurements which show the different effects on the intergrain and intragrain current transport.

Preparation of the polycristalline $(Bi,Pb)_2Sr_2Ca_2Cu_3O_{10+\delta}$ samples was done by the powder in tube technique. The mixed and calcined oxide powders were filled into silver tubes. After swageing, drawing, and rolling, tapes of 100 μm in thickness and a width of about 2.4 mm were obtained. A detailed description of our preparation techniques is given in previous papers [1 - 3]. The dimensions of the superconducting core were typically 19 μm in thickness and 1.9 mm in width. Irradiation of the samples was performed at the low-temperature facility of UNILAC using 2.65 GeV ^{197}Au-ions as projectiles. During irradiation the samples were maintained at a temperature of approximately 100 K. Great care was taken, to achieve an homogeneous damage production throughout the sample volume.

Critical current densities j_{cm} were magnetically determined from the width of the irreversible magnetization loops ΔM in accordance with the Bean model. Temperature dependent j_{cm} - measurements are displayed in Fig. 1. One can see a marked enhancement of j_{cm} after irradiation in the whole temperature range especially for B-fields less than the dose equivalent fild of $B_\phi = 2$ T for a dose of 1.0 x 10^{11} ions/cm^2. This j_{cm} - enhancement is caused by the additional pinning centers created in the superconducting grains by heavy ion irradiation. Similar results were found in j_{ct} - transport measurements as plotted in Fig. 2, when B is applied in parralel to the tracks. Although the intergrain transport current is much smaller than the intragrain current there is also an enhancement of j_{ct}. We found drastic j_{ct} - improvements similar to those observed for j_{cm} at elevated temperatures like 60 K and 77 K after irradiation. The thermally activated depinning of pancake vortices was reduced by very effective columnar pinning centers. According to Fig. 3 j_{ct} - enhancement is also evident in the same temperature range for the field applied perpendicular to the ion tracks and for magnetic fields B larger than 1 T. In this case B is directed perpendicular to the average c-axis direction of the individual grains having a misalignment of $\pm 10°$. The field component $B_{\|c} = B \sin 10°$ parallel to the c-axis of the individual grains generates pancake vortices and the thermally activated motion of these vortices is consequently reduced to the columnar defects, intersecting the a-b-planes. At lower temperatures one can find a only slight decrease of j_{ct}. For these temperatures the thermal activation is much smaller and the additional introduced defects are not more efficient than the intrinsic ones. The small j_{ct} - reduction can be attributed to the introduced damage fraction which was calculated to about 8% for 1.0 x 10^{11} ions/cm^2 and a track diameter of 10 nm.

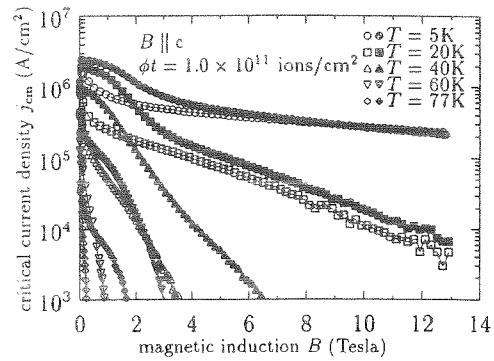

Fig. 1: j_{cm} from magnetization measurements versus magnetic induction B for 2223 BPSCCO tapes before (open) and after (closed) irradiation with gold ions.

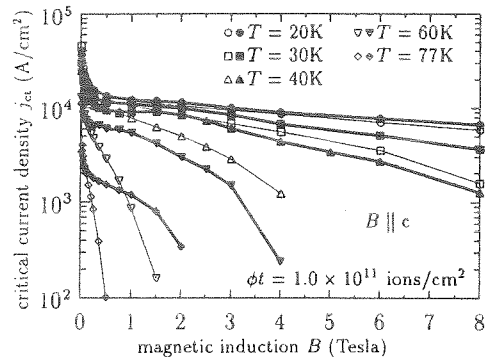

Fig. 2: Critical current density j_{ct} versus magnetic induction B for 2223 BPSCCO samples before (open) and after (closed) irradiation with 2.65 GeV ^{197}Au-ions for B || c.

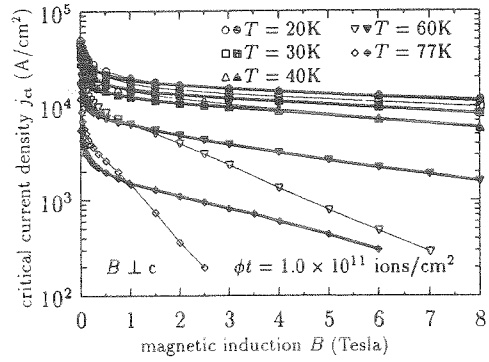

Fig. 3: Critical current density j_{ct} versus magnetic induction B for 2223 BPSCCO samples before (open) and after (closed) irradiation with 2.65 GeV ^{197}Au-ions for B $\perp$ c.

REFERENCES

[1] H.-W.Neumüller, W.Schmidt, M.Wilhelm, U.Härlen, G.Hofer, W.Kleinlein
Proc. 5th Int. Symp. on Superconductivity, Kobe, Japan, Nov. 16-19, 1992 (1993) p. 811

[2] M.Wilhelm, H.-W.Neumüller, G. Ries
Physica C 185-189 (1991) p. 2399

[3] H.-W.Neumüller, M.Wilhelm, K.Fischer, A.Jenovelis, M.Schubert, C.Rodig
ICMC, July 12-16, 1993, Albuquerque, New Mexico, USA

Fast solvent extractions with SISAK 3 as a test for chemical studies of element 106[B]

K. Eberhardt[1], G. Herrmann[1], A. Nähler[1], M. Pense-Maskow[1], N. Trautmann[1], B. Wierczinski[1]
G. Skarnemark[2], J. Alstadt[3], B. Eichler[4], H. Gäggeler[4], D. Jost[4], A. Türler[4], A.V.R. Reddy[5]
[1]Institut für Kernchemie, Universität Mainz; [2]Chalmers University of Technology, Göteborg
[3]Department of Chemistry, University of Oslo [4]Paul Scherrer Institut, Villigen
[5]Bhabha Atomic Research Center, Trombay

For studies on the chemical behaviour of the transactinide elements fast and -if possible- continuous chemical separation procedures are required. The development of such procedures based on liquid-liquid extractions have been performed with the lighter homologues of the transactinide elements using the fast centrifuge system SISAK 3 [1].

Carrier-free isotopes of Zr, Nb, Mo and La have been produced by thermal neutron-induced fission of Pu-239 at the TRIGA Mainz Reactor and those of Hf and W in bombardment of Hf- and W-foils with 49 MeV α-particles at the PSI, Villigen. The reaction products were transported to the SISAK centrifuges by means of a gas-jet transport system. The extraction yields were determined by simultaneously measuring the γ-ray activity of the aqueous and the organic phase. Different detector cells can be used to adjust the hold-up time in front of the detector with respect to the half-life of the nuclide to be studied.

For the investigation of the chemical behaviour of element 106 several extraction systems have been studied and three of them seem to be best suited:

- Aliquat 336/Toluene — HCl
- TOPO/Shellsol T — HCl
- TOA/Shellsol T (or Toluene) — α-HIB

In figure 1 the extraction yield of Mo, W, Nb, Zr, Hf and La is plotted as a function of pH-value for TOA(2% by volume in Shellsol T)/1 M α-HIB. At the pH-value of the unbuffered acid (pH$\approx$1.8) the extraction yields for Mo and W are 85 %. Nb (as a homologue for element 105) is also extracted to approx. 70 % over a wide range of pH-values. Within the error limits extraction of La, Zr and Hf into the organic phase is negligible. Lactic acid instead of α-HIB can be used as complexing agent as well. In the TOPO/HCl–system extraction yields of 80 % were obtained for Mo and W at HCl-concentrations higher than 5 M. At such concentrations Hf is extracted to more than 40 %. In the case of Aliquat 336/HCl the extraction yields for Mo and W are better than 90 % from 6 M HCl, but under these conditions Zr is extracted to approx. 20 % and the extraction of Hf also starts. This could cause problems with element 104 as a daughter product of element 106.

For on-line α- and spontaneous fission measurements of transactinide elements a liquid scintillation counter (LSC) has been developed and tested [2] using dimethyl-POPOP as a scintillator together with naphthalene in toluene. In the TOPO/HCl–system no phase separation can be achieved with toluene as the organic solvent at the optimum extraction conditions for Mo and W. With Aliquat 336/HCl the scintillator precipitate when the organic phase is contacted with HCl at higher acid concentrations. Only the TOA/α-HIB (or lactic acid)–system is suitable for studies of the chemical properties of element 106 in combination with SISAK 3 and the LSC-detector. Here, the extraction yield is not affected with toluene as a solvent and in the presence of dimethyl-POPOP and naphtalene.

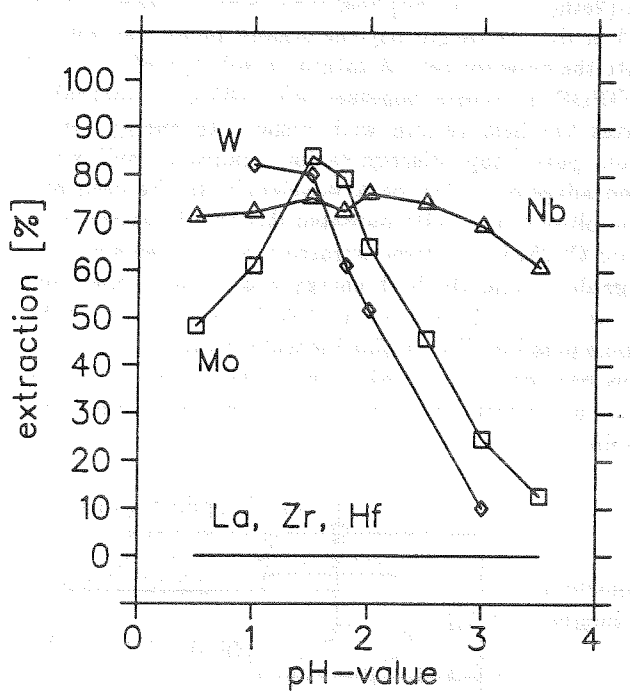

Figure 1: *Extraction of the homologues of the elements 103, 104, 105 and 106 with trioctylamine (TOA) as extractant (2 % by volume in Shellsol T) and 1 M α-hydroxyisobutyric acid (α-HIB) as the aqueous phase in dependance on pH-value*

References:

[1] H. Persson et al., Radiochimica Acta 48, 177 (1989)
[2] B. Wierczinski et al., contribution to this report

A liquid scintillation detector for on-line α- and spontaneous fission measurements[B]

B. Wierczinski[1], K. Eberhardt[1], G. Herrmann[1], M. Mendel[1], A. Nähler[1], U. Tharun[1], N. Trautmann[1], N. Wiehl[1], G. Skarnemark[2], J. Alstadt[3], B. Eichler[4], H. Gäggeler[4], D. Jost[4], A. Türler[4]

[1]Institut für Kernchemie, Universität Mainz; [2]Chalmers University of Technology, Göteborg

[3]Department of Chemistry, University of Oslo; [4]Paul Scherrer Institut, Villigen

In order to study the chemical properties of the transactinide elements with the fast, continuous solvent extraction system SISAK 3 [1], on-line spectroscopy of α-particles and SF fragments in solution is necessary. To meet this requirement a new detection system based on liquid scintillation counting (LSC) [2] has been developed for measurements in a flowing liquid. For this an extractive scintillator consisting of a scintillator, naphthalene and an extracting agent for the separation of the desired element, all dissolved in toluene is used.

In off-line tests the performance of different scintillators, among them 2–(4'–biphenyl)–6–phenylbenzoxazol (PBBO) and dimethyl[2,2'–p–phenylbis(4–methyl–5–phenyl)oxazol] (dimethyl-POPOP) dissolved in toluene or p-xylene has been investigated with the α-emitters U-233 and Am-241. Both isotopes were extracted with di-(2ethylhexyl)-orthophosphoric acid (HDEHP) from 0.1 M HCl. Subsequently the organic phase was injected into the detector cell. A saturated solution of dimethyl-POPOP in toluene together with 160 g/l naphthalene gives the best results with respect to energy resolution, pulse-shape-discrimination against β- and γ-rays and adaption of the peak wavelenght to the used photomultiplier tube (Hamamatsu R2014). In experiments with Cf-252 it was demonstrated that SF-events produce signals beyond the high energy end of the α-spectrum. Thus, α-particle–SF time correlation measurements become possible. For on-line measurements a detector cell has been constructed which is shown in Fig. 1. It consists of a quartz cell, a teflon reflector and a photomultiplier tube.

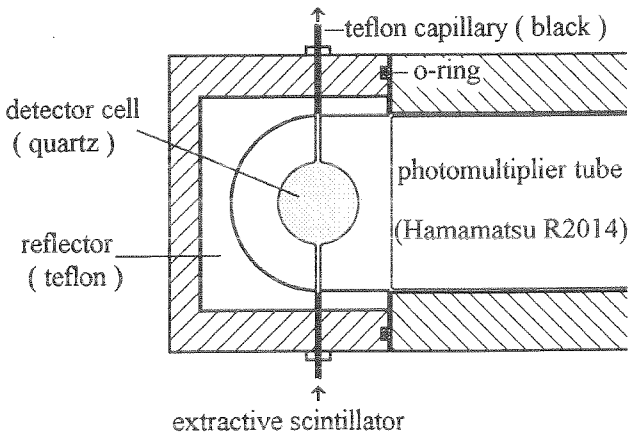

Figure 1: *Schematic drawing of the detector cell used for liquid scintillation counting.*

In test experiments, an aqueous solution of U-233 and Am-241 (0.01 M HCl) was contacted with an extractive scintillator with HDEHP as the extracting agent in SISAK 3. The isolated organic phase was pumped with a flow rate of 0.5 ml/s through a 3 ml detector cell. A resolution of 213 keV at 4.8 MeV has been achieved (see Fig. 2)

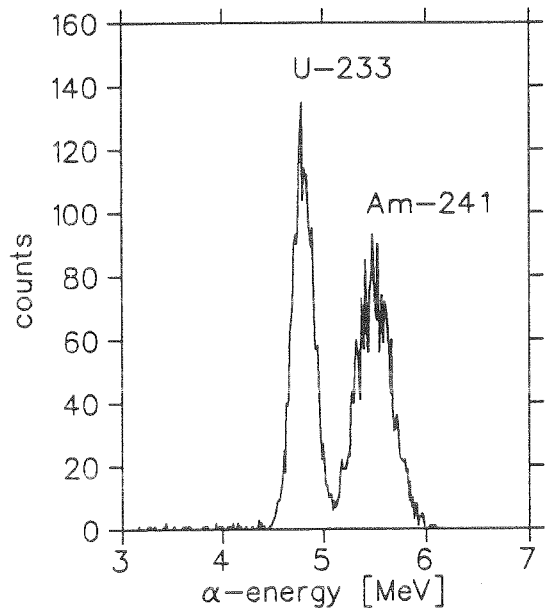

Figure 2: *On-line α-Spectrum of U-233 and Am-241 after extraction with HDEHP. A resolution of 213 keV at 4.8 MeV is achieved in a flowing liquid.*

As a further test, α-particle emitting neutron-deficient isotopes of uranium, protactinium and thorium have been produced in the bombardement of thorium with 120 MeV α-particles at PSI, Villigen. The activities, transported with a gas-jet and afterwards dissolved in 0.1 M HCl, were extracted with HDEHP into the scintillator solution. The experiments show that in the presence of a large surplus of β- and γ-radiation pulse-shape-discrimination is irrevocable for α-particle measurement with good energy resolution. Furthermore an event by event registration has been applied to establish mother-daughter correlations.

References

[1] H. Persson et al., Radiochimica Acta 48, 177 (1989)

[2] W.J. McDowell: Alpha Counting and Spectrometry Using Liquid Scintillation Methods, Report NAS-NS-3116 (1986)

Sorption Studies of Subgroup IV, V and VI Elements on Ion Exchangers from Weak HCl/HF Solutions. Model Experiments for the Separation of Element 106 G,B

D. Schumann,[1] S. Fischer,[1] St. Taut,[1] R. Dressler,[1] A. F. Novgorodov,[2] R. Misiak,[3] N. Trautmann,[4] M. Schädel,[5] H. Bruchertseifer [6]

[1]FG Radiochemie, TU Dresden, BRD, [2]Lab. f. Kernprobleme, JINR, Rußland, [3]Inst. f. Kernphysik, Krakow, Polen, [4]Inst. f. Kernchemie, Universität Mainz, BRD, [5] GSI Darmstadt, BRD, [6]PSI Villigen, Schweiz

Studies of element 106 require in the first step a sufficiently high separation of the unwanted actinides and transactinides. For such a separation we propose a cation exchange procedure from HCl/HF acid solution partly in analogy to investigations of element 104[1,2]. For the separation of element 106 we studied the sorption behaviour of the tracers ^{89}Zr, ^{181}Hf, ^{182}Ta, ^{99}Mo, ^{178}W and the pseudo-subgroup V element ^{233}Pa on DOWEX 50x8 from HCl/HF solutions.

^{182}Ta and ^{181}Hf were produced by irradiating metallic Ta and $^{180}HfO_2$ at the IBR2 reactor (Laboratory of Neutron Physics, JINR Dubna). Details of sample preparation are given in [3].
^{99}Mo was obtained by eluting a commercial $^{99}Mo/^{99m}Tc$ generator with 5 vol % NH_4OH solution. The eluate was evaporated to dryness and the activity dissolved in 0.1 M HCl.
^{178}W was produced by bombardment of metallic Ta with 650 MeV protons at the phasotron "P" (Laboratory of Nuclear Problems, JINR Dubna). Tungsten was separated from the irradiated target by thermochromatography using moist air and subsequently dissolved in 0.5 M HCl.
^{233}Pa was produced by neutron irradiation of thorium nitrate at the TRIGA Mainz reactor. After the solution of the target in 9 M HCl Pa was adsorbed on an anion exchange column and eluted with 4 M HCl.
^{89}Zr was obtained by irradating Y_2O_3 with protons at the cyclotron in Jülich (Inst. f. Nuklearchemie, KFA Jülich GmbH). The target was dissolved in 6 M HCl and after its adsorption on Dowex 1x8 the Zr was eluted with 4 M HCl.
The sorption studies were carried out by batch experiments. For this 5 ml of the radioactive solution were contacted with 200 mg DOWEX 50x8 (20-50 mesh) for one hour. The γ-activity of the aqueous phase was measured before and after the experiments.

The distribution coefficients D of Zr, Hf, Pa, Ta, W and Mo on DOWEX 50x8 in dependence on the HCl concentration in the presence of 10^{-3} M HF are shown in fig. 1. At concentrations lower than 0.1 M HCl Zr and Hf are completely adsorbed on the cation resin, while Mo shows a K_D of ~10 and W of ~3. From these values a partial sorption of W and Mo in column experiments is expected, but on-line experiments showed, that both elements completely pass through the cationic column using 0.05 M HCl/10^{-3} M HF and flow rates of ~ 2 ml/min.[5]. HCl concentrations higher than 0.1 M HCl are not recommended because the sorption of subgroup IV elements, actinides and lanthanides decreases[6]. Pentavalent elements cannot be separated from the hexavalent in this way.
If the HF concentration is lowered to 10^{-4} M the sorption behaviour of the described elements depends on the HCl concentration in the following way (fig. 2): Up to a concentration of 0.1 M HCl tetra- and pentavalent elements remain on the cation exchanger, while Mo and W are not or only slightly adsorbed.

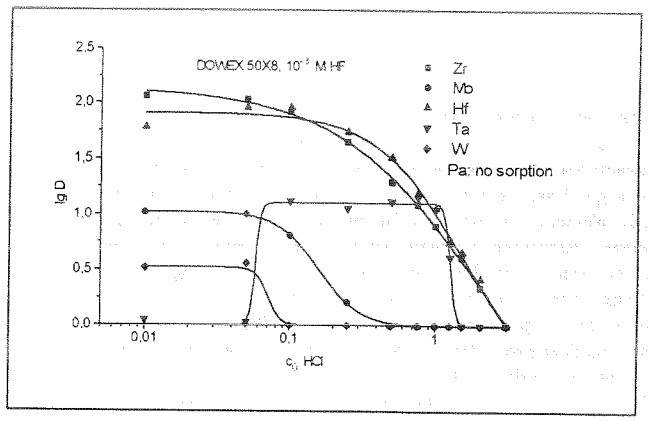

Fig. 1: Distribution coefficients D on DOWEX 50x8 in dependence on HCl concentration in solutions containing 10^{-3} HF

However, sorption experiments on the anion exchanger DOWEX 1x8 showed that the investigated tetra- and pentavalent elements are also adsorbed with high distribution coefficients. This could be caused either by hydrolysis or the formation of none charged compounds, the later being adsorbed on several surfaces.These effects are difficult to control and not well reproducible. Therefore, for the separation with ARCA III[4] a 0.05 M HCl/10^{-3} M HF solution is recommended.

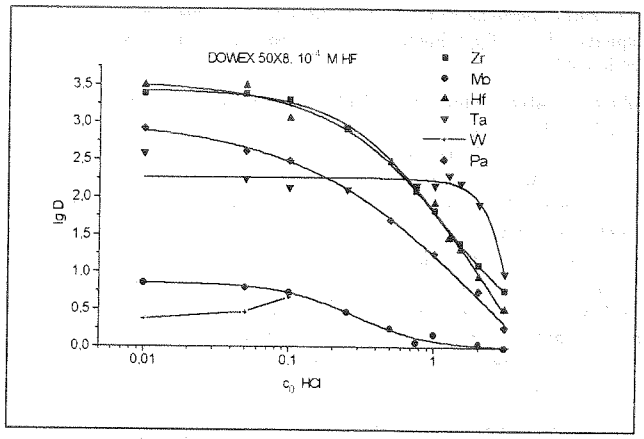

Fig. 2: Distribution coefficients D on DOWEX 50x8 in dependence on HCl concentration in solutions containing 10^{-4} HF

References

[1] H. Bruchertseifer et. al. Radiochim. Acta **47**(1989) 41
[2] Z. Szeglowski et. al. Radiochim Acta **51**(1990) 71
[3] D. Schumann et. al. J. Radioanal. Nucl. Chem. Lett. in press
[4] M. Schädel et. al. Radiochim. Acta **48** (1989) 171
[5] D. Schumann et. al., Dubna Report 1993, in print
[6] M. Marhol, Ion Exchangers in Analytical Chemistry, Academia, Prague, 1982

Extractions and Separations of Molybdenum in Model Experiments for Chemical Separations of Element 106

H.U. Becker, J.V. Kratz
Institut für Kernchemie, Universität Mainz

W. Brüchle, M. Schädel
GSI, Darmstadt

In the preparation of our planned experiments on element 106, we have studied a variety of extraction systems which potentially can characterize the chemical behaviour of element 106, and which allow a good separation of element 104 and trivalent actinides. Most likely element 105 will not be produced with an appreciable cross section. Assuming a similar chemical behaviour, separations of the lighter homologues have been tested. The homologues lanthanum, yttrium, zirconium, niobium and molybdenum were obtained carrier-free as fission products of uranium at the TRIGA-reactor in Mainz. The chemical properties of element 106 in aqueous solutions will presumably be studied with the Automated Rapid Chemistry Aparatus ARCA [1], and, as a complementary method, with the fast centrifuge system SISAK [2].

In the first experiments, the distribution of tracer activity in the aqueous and the organic phase was determined by batch-wise liquid-liquid extraction experiments. 3 ml of the organic phase and 3 ml of the aqueous phase were shaken for 20 s. After the phase separation aliquots of 2 ml were taken from each solution, and the γ-activity was measured.

The extraction of La, Y, Zr, Nb and Mo has been tested in various extraction systems with HCl concentrations between 0.01 M and 12 M and HNO_3 concentrations between 0.01 M and 14 M as the aqueous phase. As the organic phase we examined tricaprylmethyl-ammoniumchloride (Aliquat-336)/$CHCl_3$, bis(2-ethyl-hexyl)-phosphate (HDEHP)/toluene, tributylphosphate (TBP)/toluene, trioctylphosphinoxide (TOPO)/toluene or trioctylamine (TOA)/toluene.

In all investigated systems the trivalent compounds of La and Y, studied as homologues of the actinides, were not observed in the organic phase above 1 M HCl as the aqueous phase. We observed the best separation of Mo from the other elements in a system of 10% TOA in 90% toluene. Here molybdenum,the homologue of element 106, is completely extracted into the organic phase at HCl concentrations of 3 molar and higher, see Fig. 1. Zirconium is extracted only in 12 M HCl. The extraction of niobium starts between 3 and 4 M HCl.
With HNO_3 as the aqueous phase molybdenum was found in the aqueous phase between 0.5 M and 10 M HNO_3. Consequently, we shall be able to reextract molybdenum back into the aqueous phase under these conditions.

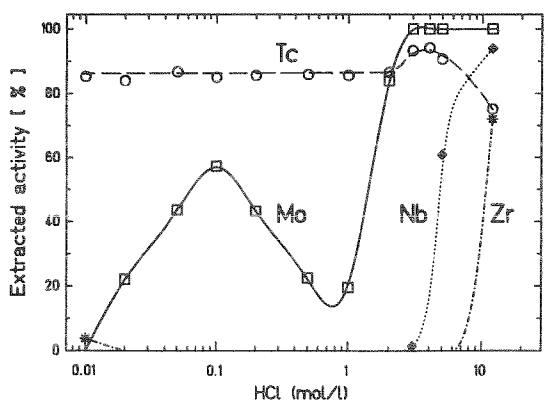

Fig. 1: Liquid-liquid extraction of Mo, Nb, Zr, La and Y into TOA/toluene. Only values above 1% in the organic phase are shown.

In further experiments the result of the liquid-liquid extraction experiments was applied in chromatographic separations as a test for the ARCA. As the stationary phase in our chromatographic column (1.6mm i.d., 25mm long) we used TOA on Voltalef (63-126 mesh) as an inert support. The flow rate of the mobile aqueous phase was kept at 1 ml/min.

In these experiments HCl solutions of various concentrations were tested to load the Mo onto the resin. The best results were obtained at 5 M HCl. At this concentration niobium, zirconium, yttrium and lanthanum were eluted within $\sim$ 500 μl while molybdenum was retained completely on the column. Contrary to our expectations from the liquid-liquid extraction experiments, see Fig. 1, we did not observe a complete elution of Nb below 5 M HCl. Above 5 M HCl we may loose some Mo while loading the column.

The elution of molybdenum with concentrations lower than 1 M HCl was not successful contrary to our expectations from the batch experiments.
An almost quantitative elution of Mo was possible with 2 M HNO_3. Figure 2 depicts the elution curve. It shows that La, Y and Zr were completely and more than 90% of Nb was eluted within 500 μl of 5 M HCl. A Mo fraction with a yield of 90% can be eluted within 500 μl of 2 M HNO_3. It contains about 5% of Nb.
From these experiments we found in the system TOA/toluene with 5 M HCl and 2 M HNO_3 as the aqueous phases, good conditions under which we can expect to isolate a clean fraction of element 106 in ARCA. This system has also the potential for a further detailed investigation of the chemical properties of element 106 as a member of group 6 of the periodic table of elements.

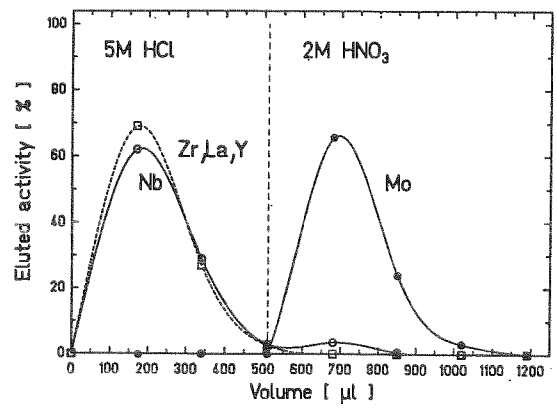

Fig. 2: Chromatographic separation of Mo as the lighter homologue of element 106 from Nb, Zr, La and Y on a TOA/Voltalef column.

[1] M. Schädel et al., Radiochim. Acta 48, 171 (1989)
[2] H. Persson et al., Radiochim. Acta 48, 177 (1989)

A Chemical Separation Procedure to Search for ^{263}Rf in a Possible EC-Decay of ^{263}Ha

W. Brüchle, M. Schädel, B. Schausten, E. Schimpf
GSI Darmstadt
R. Günther, U. Becker, J.V. Kratz, N. Trautmann
Institut für Kernchemie, Universität Mainz

The unknown isotope, ^{263}Rf will have lower Q-values for both EC and α decay than all other known isotopes of element 104, Rf. If the Spontaneous Fission (SF) half-life is sufficiently long, the overall half-life of ^{263}Rf could be at least several minutes. An element 104 isotope with such a half-life would make more detailed studies of the chemical properties of element 104 possible. As the production rates of ^{263}Rf in reactions like $^{248}Cm(^{18}O, 3n)$ are very small, we developed a chemical procedure to search for ^{263}Rf as a possible EC-decay daughter of ^{263}Ha.

In a series of earlier experiments we identified the new isotope ^{263}Ha [1,2]. These experiments involved the chemical separation of a Ha fraction by elution from a cation exchange column with α-hydroxyisobutyrate (BUT) solution [2]. Based on this separation we have studied an extended procedure which allows a sequence of five collection and separation cycles of a Ha fraction on one column. As a typical time for each cycle can be one minute, we can collect the Ha decay products for five times one minute. While the Ha is eluted immediately after each collection cycle, tetravalent ions, including element 104, are retained on the chromatographic column under the optimized conditions. After having eluted the fifth Ha fraction we were aiming to specificly elute the tetravalent ions and element 104, if present, from the column without any interference from trivalent actinides.

We have developed and tested such a procedure with tracer activities of the lighter homologues. Carrier free Nb, Zr, and lanthanides, produced as fission products at the TRIGA Mainz reactor, and transported with a He(KCl) jet to the Automated Rapid Chemistry Apparatus [3], ARCA, served as tracers to simulate the behaviour of the elements 105, 104 and the actinides. In addition, Tm, activated at the Mainz Triga reactor and commercially available Y-tracer were used to characterize the behaviour of the heavier actinides.

On our typical cation exchange column (1.6 mm i.d., 8 mm long), filled with (17.5 $\pm$ 2) μm Aminex A6 resin, we could carry out five one-minute collection and separation cycles of a Ha fraction with unbuffered 0.05 M BUT. We have tested this procedure for Ha fraction sizes between 85 and 170 μl; each fraction eluted within 5 to 10 s with a rate of 1 ml/min. Under these conditions, all tri- and tetravalent ions are strongly retained on the cation exchange resin.

A variety of eluents to specificly elute a clean fraction of element 104 were tested in experiments with Zr tracer.

In our first attempts we eluted Zr with unbuffered 0.5 M BUT. Within 150 μl 87 % of the Zr was eluted, and no activity of any lanthanide tracer was detectable.

As an alternative eluent we also tested 0.01 M and 0.1 M HF. With the 0.01 M Hf solution no quantitative elution of Zr was possible, and a fraction of 170 μl contains only 35 % of the Zr. The 0.1 M HF is a much better choice. About 87 % of the Zr was eluted within 120 μl, and about 93 % within 170 μl. All these fractions are very clean, and no interference was detectable from the trivalent actinide equivalent lanthanides.

We have applied the separation scheme with the 0.1 M HF in an experiment to (i) continue the investigation of the α- and Spontaneous Fission (SF) decay properties of ^{263}Ha, and to the search for an EC-decay branch of ^{263}Ha into the unknown isotope ^{263}Rf in the ^{18}O + ^{249}Bk reaction at 93 MeV. For the Rf fraction we chose an elution time of 8.5 s from which we approximately obtained a 90 % chemical yield for tetravalent ions in a 142 μl fraction. The α- and SF-decay measurements with a series of ten Passivated Implanted Planar Silicon detectors started 40 s after end of irradiation while the measurement of the Ha fraction started 30 s after end of irradiation. Presently the measured data are under evaluation.

References

[1] J.V. Kratz et al., Phys. Rev. C45, 1064 (1992)

[2] M. Schädel et al., Radiochim. Acta 57, 85 (1992)

[3] M. Schädel et al., Radiochim. Acta 48, 171 (1989)

Investigation of the transport efficiency of a He(KCl) gas jet for heavy ion reaction products[B]

R.Günther[1], A.Weber[1], H.U.Becker[1],A.V.R. Reddy[1], J.V.Kratz[1]
M.Schädel[2],W.Brüchle[2], E.Jäger[2], E.Schimpf[2], B.Schausten[2]
[1] Institut für Kernchemie Universität Mainz, [2] GSI Darmstadt

An efficient, fast and reliable transport of recoiling evaporation residues is a prerequisite for heavy element research with chemical techniques. In order to improve the transport efficiency of our He(KCl) gas jet, test experiments were performed at the GSI and at the MPI für Kernphysik in Heidelberg. The response of our gas jet to changes of a variety of parameters was investigated with heavy ion beams. The reaction used for this investigation at the MPI was $^{181}Ta(^{12}C,xn)^{189-192}Au$ with a beam energy of 77 MeV. These Au-isotopes have approximately the same recoil ranges as heavy elements produced in actinide based reactions. To study the properties of the KCl-particles, e.g. their diameter and number concentration, we used the DMPS/C-system[1] and the transported activity was examined by γ-spectroscopy.
The most important parameters affecting the aerosol generation are the helium flow, the pressure in the furnace and the furnace temperature. The beam intensity was kept at 10 nA (DC) for these parameter studies. Increasing the furnace temperature leads to an increase of the mean geometric diameter, D_g, of the KCl aerosol particles. The particle concentration increased slowly while the yield did not change significantly.

Temp. °C	D_g nm	Particle $1/cm^3$	Yield %
644	235	$6.0 \cdot 10^5$	52
660	263	$6.1 \cdot 10^5$	57
684	294	$6.4 \cdot 10^5$	55

Table 1: Temperature dependance of the yield

The transport yield was also constant while the pressure in the recoil chamber was varied from 1.26 bar to 1.7 bar.
Increasing the helium flow from 0.6 l/min to 2.8 l/min leads to an increase of the transport yield (Fig. 1) and of the particle concentration.

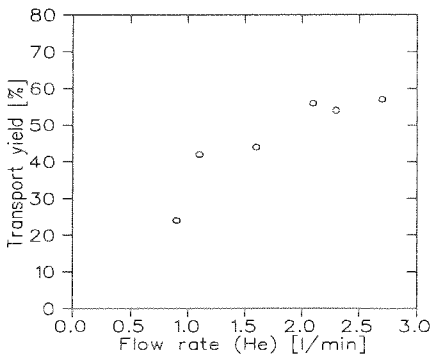

Fig. 1: The transport yield as a function of the He-flow rate

When we increased the beam intensity from 16 to 1450 nA (AC) we observed a decrease of the transport yield.

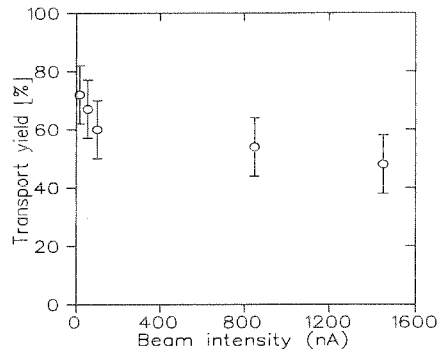

Fig. 2: The transport yield as a function of the beam intensity

The heavy ion beam is also altering the particle diameter. At low current (16 nA) D_g was enlarged compared to the diameter without an ion beam in the target chamber. At higher beam currents D_g was reduced again but it remained slightly larger than the original diameter without any ion beam. The cause of this increase can be explained by the enhanced coagulation due to the electrostatical attraction force of highly charged particles[2]. Calculations[3] made at GSI show a high electron density (about 10^6 electrons per cm^3) in the He of the recoil chamber under typical conditions to investigate heavy elements. This leads to a bipolare charge distribution of the aerosol particles passing the target chamber. The proof of positively charged particles could be made with the DMPS/C system. The bipolar charger (^{85}Kr source) was removed from the system and thus positively charged particles out of the gas jet system could be classified and detected. A particle distribution was found corresponding to the one measured with the charger. This indicates a Boltzmann distribution of positively charged particles. After having installed a bipolare charger after the target chamber to convert the existing charge distribution to a Boltzmann type, an increase of the transport yield of 20 % was observed. The loss of the KCl aerosol particles on the wall of the recoil chamber due to their high mobility can also contribute to the losses in transport yield. Therefore a variable positive and negative voltage was applied to the aerosol sampling cup inside of the recoil chamber. Low voltages (10 - 200 V) did not affect the yield. Higher voltages reduced the yield. The electrostatical and hydrodynamical properties inside the chamber were changed by inserting various shaped and sized sampling cups to find the optimum insert. While we studied the influence of the capillary length on the yield we found no sgnificant reduction over the first 10 m and a about 20% lower yield after 20 m.

References

[1] R. Günther, Institut für Kernchemie Jahresbericht 1992, 1
[2] W.C.Hinds, Aerosol Technology, Wiley&Sons, New York, 240
[3] P. Strehl, priv. comm., 1993

Extraction of Zr,Nb,Ta,Pa, and Np into Triisooctyl Amine from pure HCl solutions [B]

W.Paulus, H.P.Zimmermann, S.Zauner, J.V.Kratz
Institut für Kernchemie der Universität Mainz

We have previously studied [1,2] the extraction of M^{4+} and M^{5+} ions into triisooctyl amine (TiOA) from aqueous solutions of various HCl concentrations containing typically 0.03 M HF. This relatively small amount of HF is known [3] to greatly stabilize the behaviour of Nb, Ta, and Pa in aqueous solutions. In order to avoid hydrolysis and polymerization, the radioactive tracers of these elements and of Zr and Hf were generally stored in fluoride-containing solutions [1]. Then, if their extraction behaviour in " fluoride-free" mineral acids was to be studied, boric acid was added to the aqueous solutions prior to the batch extraction.

According to thermodynamics [4], through formation of the extremely stable BF_4^-, this should destroy the fluoride complexes of the metal ions. For Nb, Ta, and Pa, however, there was little difference in the extraction behaviour from "fluoride-free" HCl and HCl/HF mixtures [1] which was in conflict with some literature data. The latter are not considered [3] firmly established. Therefore, we have reexamined the system TiOA/HCl, whereby the presence of HF was consequently avoided. Fig. 1 shows the extracted activity of Pa, Nb, and Zr from HCl solutions. Under these conditions, the behaviour of Np^{5+} is largely identical to that of Nb^{5+}. Ta^{5+} was not extracted. As ^{182}Ta from ^{181}Ta (n,γ) reaction was used as a non carrier-free tracer, polymerization is considered to cause this behaviour, as it is in conflict with the previously observed complete extraction from 10 M HCl of carrier-free Ta^{5+} freshly produced at an accelerator [1]. Fig.1 shows that the extraction from intermediate HCl concentrations of Pa is more effective than that of Nb which is the reversed order compared to the extraction from HCl/0.03 M HF; also the local extraction maximum [1,2] at 0.5 M HCl/0.03 M HF is not present in the pure TiOA/HCl system. Thus, the previously observed similarity of the extraction of Nb, Ta, and Pa into TiOA from HCl/HF or from " fluoride-free" HCl solutions is an artifact, and the destruction of the fluoride complexes of the tracers by boric acid did not work, apparently. In order to check this further, we have added 0.03 M HF to the HCl solutions prior to the extraction into TiOA: This reproduced the well-known [1] sequence of extraction Ta>Nb>Pa with the local maximum extraction of Nb and Pa at 0.5 M HCl/0.03 M HF and a minimum at 4 M HCl/0.03 M HF.

Also in agreement with the previous studies [1], Zr was not extracted, even from 12 M HCl/0.03 M HF. The addition of a surplus of H_3BO_3 at 70° C for up to three hours prior to the extraction did not change these results back to the behaviour displayed in Fig. 1, except for Zr. Thus, we have to conclude that, in the presence of fluoride ion, Ta, Nb and Pa, but not Zr, from kinetically stable fluoride complexes or mixed chloride/fluoride complexes that cannot be destroyed by boric acid contrary to the expectation [4]. In particular, for non carrier-free Ta, the non-extractable polymeric ions change to extractable monomeric forms by the addition of HF. In 10 M HCl this was studied by measuring the distribution coefficient K_D as a function of HF molarity: There is no extraction at $< 10^{4-}$ M HF and a steep rise (K_D=15 at $5\times10^{4-}$ M HF; K_D= 80 at 10^{3-} M HF) for higher HF molarities. In conclusion, in the experiments carried out with carrier-free Nb, Ta, Pa, and element 105 [1,2], the presence of fluoride ion played an important role and mixed oxo or hydroxo complexes such as $[MOCl_xF_y]^{x+y-3}$ or $[M(OH)_2Cl_xF_y]^{x+y-3}$ must have been present for Nb, Pa, and element 105, while Ta must have been present as $[TaCl_xF_y]^{x+y-5}$ with x and y resuming a multitude of values. As the stoichiometry of the pure chloride complexes in pure HCl solutions is better defined, we envisage future experiments with Nb, Ta, Pa, and element 105 in the absence of fluoride ion. To prepare these, we have performed chromatograhic separations using columns of ARCA dimension (1.6x8mm) filled with TiOA on an inert support (Voltalef, 32-63 μm). As suggested by the extraction data shown in Fig. 1, tracers of Eu^{3+}, Zr^{4+}, Nb^{5+}, Pa^{5+}, and Np^{5+} were fed onto the column from 10 M HCl/0.01 M HNO_3 (HNO_3 is needed to stabilize pentavalent Np), Zr was eluted in 6 M HCl/0.01 M HNO_3, Nb and Np in 3.5 M HCl, and Pa in 0.5 M HCl. It appears that, in principle, these separations should be highly suitable to characterize the chloride complexing of element 105 relative to that of its homologs. The behaviour of Ta could not yet be checked as no carrier-free Ta tracer was available. However, there is a general problem associated with theses TiOA/HCl column separations, i.e. a very slow extraction and back extraction kinetics. We plan to continue partition and column experiments with fluoride-free HCl solutions and other anion exchangers in order to find a system in which the kinetics is acceptable.

[1] J.V.Kratz et al., Radiochim. Acta 48, 121(1989)
[2] H.P.Zimmermann et al., Radiochim.Acta 60, 11 (1993)
[3] J.Korkisch, Handbook of Ion Exchange Resins, Vol.IV,CRC Press 1989, p.257
[4] L.G.Sillen, A.E.Martell, Stability Constants of Metal-Ion Complexes, Special Publication No.17, London: The Chemical Society, Burlington House,W.1 (1964)

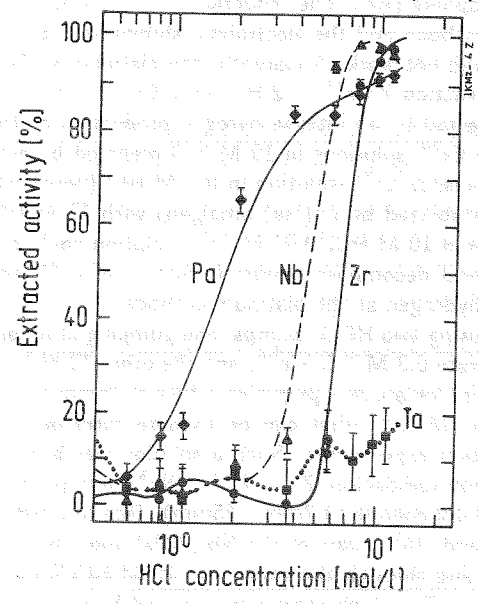

Fig.1: Extracted activity of Pa, Nb, Ta, and Zr into TiOA vs. HCl molarity. While the tracers of Pa, Nb, and Zr were carrier-free, this is not true for Ta, which forms non extractable polymeric ions [3]

Preparing Reduction Experiments with 104^{4+} and 105^{5+}

A.Hofmeister[1], W.Paulus[1], J.V.Kratz[1], M.Schädel[2], S.Zauner[1]
[1]Institut für Kernchemie der Universität Mainz
[2]Gesellschaft für Schwerionenforschung, Darmstadt

In agreement with placements in the peroidic table in groups 4 and 5, the most stable oxidation states of elements 104 and 105 are the tetravalent [1] and pentavalent [2] state, respectively. Relativistic atomic multiconfiguration Dirac-Fock (MCDF) calculations have shown that the relativistic stabilization of the s and $p_{1/2}$ orbitals in the heavy actinides and transactinides may influence the stability of oxidation states. This makes a search for lower oxidation states under reducing conditions an interesting goal of experimental investigations.
We have previously searched for a lower oxidation state in element 103, Lr [3]. There was no experimental evidence for the reduction of Lr^{3+} although in the same experiments Md^{3+} was reduced to Md^{2+}. The resulting limit for the reduction potential of the Lr^{3+}/Lr^{2+} couple was E^0 <-0.44 V. Reduction was attempted in 0.3 M HCl/0.01 M Cr^{2+} solution.
The chromous ion was prepared and stabilized by storing the solution over a bottom layer of Zn(Hg) amalgan, and the experimental technique was tested by the successful reduction of Eu^{3+} to Eu^{2+} [3].
In order to prepare reduction experiments with 104^{4+} and 105^{5+} we have studied the anion exchange of Zr^{4+}, Nb^{5+}, and Np^{5+} into the anion exchanger AG1-X8. After absorption onto the column from 10 M HCl as anionic chloro complexes, these ions can be stripped from the column in dilute HCl. 2^+ and 3^+ ions would not be sufficiently complexed in 10 M HCl and would run through the column. The preparation and stabilization of Cr^{2+} in 10 M HCl can no longer be done by using Zn(Hg) amalgan due to the dissolution of Zn. Therefore, it was attempted to do this by electrolysis. A vessel consisting of two half-cells containing platinum-net electrodes immersed in 0.3 M KCl (anode) and 10 M HCl containing chromic ion (cathode) was operated at a cathode potential of 0.5 V under inert gas atmosphere (Ar). The reduction of Cr^{3+} to Cr^{2+} at the platinum cathode and the electrolytic stabilization of the chromous ion did not work. Apparently, the platinum surface catalyzes the reaction $2\ Cr^{2+} + 2\ H^+ \rightarrow 2\ Cr^{3+} + H_2$.
This was suggested by an intense hyrogen production at the cathode. Even Cr^{2+} solutions in 10 M HCl prepared by mixing a higher molarity Cr^{2+} solution in 0.3 M HCl (previously prepared and stabilized by Zn(Hg) amalgan) with 12 M HCl to get the desired 10 M HCl/0.01 M Cr^{2+} solution could not be stabilized, and decomposed under formation of Cr^{3+} and generation of hydrogen at the platinum cathode.
Therefore, by using two HPLC pumps, one pumping at an appropriate flow rate 0.3 M HCl/Cr^{2+}, and the other 12 M HCl, through a T joint we are now preparing a flow of "metastable" 10 M HCl/0.01 M Cr^{2+} that can be used to carry out the planned reduction experiments. Such a solution was brought into contact with radioactive Zr^{4+}, Nb^{5+}, Np^{5+} and pumped through a AG1-X8 column (1.7mm x 25mm). Due to a reduction to Nb^{3+} and Np^{3+}, part of the Nb (20%) and Np(85%) activity is running through the column in 10 M HCl/0.01 M Cr^{2+}, see Fig. 1. Zr, which cannot be reduced by Cr^{2+}, and the non-reduced Nb and Np are then stripped from the column in 1 M HCl. In experiments with elements 104 and 105, we will use two anion exchange columns. The effluent (10 M HCl/0.01 M Cr^{2+}) from the first column will be mixed through a T joint with 10 M HCl/6% H_2O_2 thus reoxidizing the reduced transactinides. This solution is pumped through a second anion-exchange column where the re-oxidized transactinides are retained and Cr^{3+} runs through. Subsequently, both columns are stripped with 1 M HCl sampling the non-reducible transactinides from column 1 and the reducible transactinides from column 2.

[1] R.J.Silva et al.,Inorg.Nucl.Chem.Lett.6,871 (1970)
[2] M.Schädel et al.,Radiochim.Acta 57,85 (1992)
[3] U.W.Scherer et al.,Inorg.Chim.Acta 146, 249 (1988)

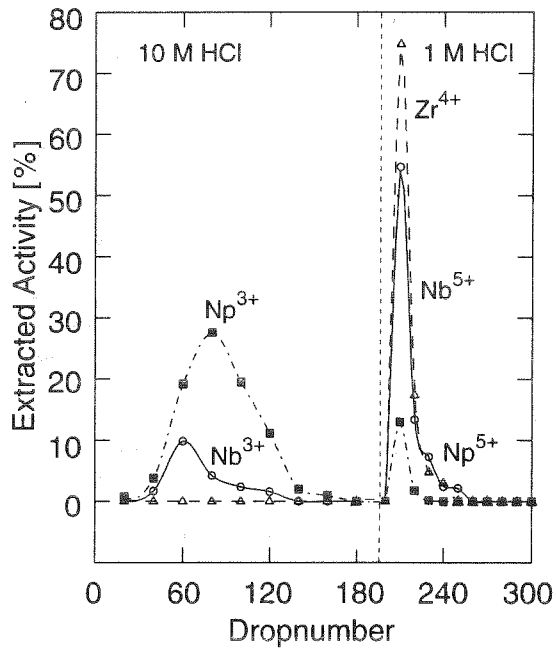

Fig.1: Elution of Nb^{3+} and Np^{3+} with 10 M HCl/0.01 M Cr^{2+} from a 1.7mmx25mm AG1X8 column at a flow rate of 1 ml/min followed by the stripping of Zr^{4+}, Nb^{5+}, and Np^{5+} in 1 M HCl

Metal-Ligand Bonding and Thermochemical Stability of Group 4, 5, and 6 Highest Chlorides

V. Pershina and B. Fricke

Theoretical Physics Department, University of Kassel

Since experimental interests are moving from halides of element 104 as a member of group 4 and of element 105 as a member of group 5 to halides of element 106, it is important to compare trends in properties of these compounds such as bonding, thermochemical stability, enthalpies of formation, etc. between the groups. From the chemistry of the 4d and 5d analogs of the transactinides it is known that the stability of the highest chlorides decreases in going to the right of the Periodic Table. Thus, to learn about the trend in the stability of the transactinide chlorides calculations of the electronic structure of MCl_4 (M = Zr, Hf, and Rf) have been performed using the Dirac-Slater Discrete Variational method in addition to the earlier calculations[1] of MCl_5 (M = Nb, Ta, and Ha) and MCl_6 (M = Mo, W, and E106).

Comparison of the results of the calculations for the three groups has shown that they are not identical with respect to the trends in electronic density distribution and bonding. $RfCl_4$ has a stronger metal-chlorine bonding than the lighter analogs since it has the highest covalency of the bond and a rather large ionic contribution. $E106Cl_6$ has a weaker bonding than WCl_6 due to the lower covalent contribution. The obtained data also confirm a very low stability of $MoCl_6$ which decomposes at the room temperature to $MoCl_5$. This compound proved to be the most ionic out of all the molecules under consideration, it has the lowest electronic density on the metal-ligand bond.

The thermochemical metal-ligand bond energies estimated on the basis of the results of the DS DVM calculations are given in Table 1.

Table 1. Average thermochemical M-Cl bond energies for the highest chlorides of groups 4, 5, and 6

MCl_4	E, kcal/mol	MCl_5	E, kcal/mol	MCl_6	E, kcal/mol
$ZrCl_4$	117.3	$NbCl_5$	97.1	$MoCl_6$	73.8
$HfCl_4$	118.4	$TaCl_5$	102.6	WCl_6	83.2
$RfCl_4$	122.9	$HaCl_5$	95.7	$E106Cl_6$	77.3

Thus, $RfCl_4$ is more stable towards thermal decomposition than the analogs, while $E106Cl_6$ is less stable than WCl_6 which is known to decompose at the boiling point equal to 346 °C.

Using estimated[2] by us ΔH_{subl} of Rf, Ha, and element 106 equal to 151.4±9, 183.5±7 and 200±6 kcal/mol, the enthalpies of formation for $RfCl_4$, $HaCl_5$ and $E106Cl_6$ have been calculated as -229.9, -150.1±7 and -90.3±6 kcal/mol, respectively. These values are shown in Fig. 1, indicating a very low stability of $E106Cl_6$, even lower than that of $MoCl_6$. Besides, these data on ΔH_{form} for the transactinides show that simple correlations of properties in groups 4, 5, and 6 do not work.

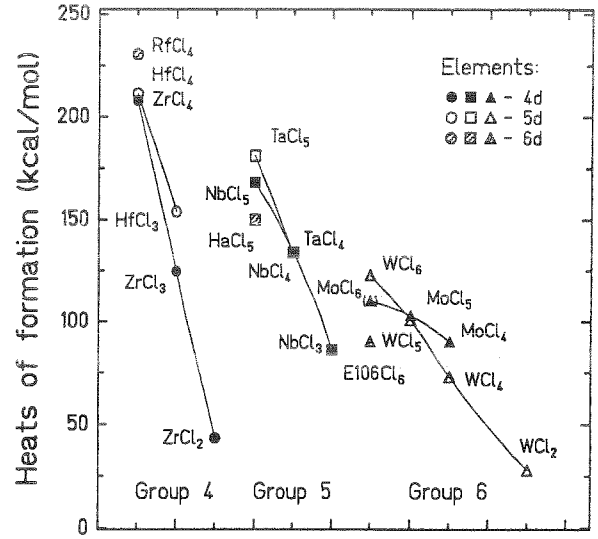

Fig. 1. Formation enthalpies of gaseous chlorides of groups 4, 5, and 6.

In addition to the decrease in the bond energy and thermodynamic stability in going from $RfCl_4$ to $E106Cl_6$, there is also a decrease in the stability of the maximum oxidation state. A correlation (Fig. 2) between the calculated energies of the charge-transfer transitions in the MCl_n molecules and standard redox potentials corresponding to transitions from the maximum to the lower oxidation state gives the values of the $E^0(E106^{6+}/E106^{5+})$ equal to -0.93 V. This shows a decrease in the stability of the maximum oxidation state Rf(+4) >Ha(+5)>E106(+6).

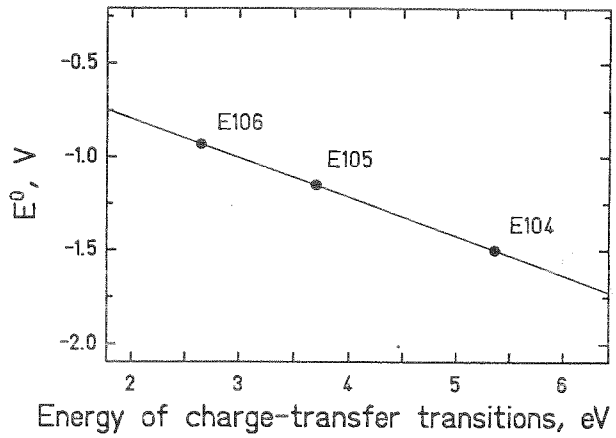

Fig. 2. Correlation between redox potentials and energies of the charge-transfer transitions in MCl_n (M = Rf, Ha, and E106).

1. V. Pershina, W.-D. Sepp, B. Fricke, A. Rosen, J. Chem. Phys. 96, 8367 (1992).
2. G. V. Ionova and V. Pershina, Sov. Radiochem., in press.

Anionic Oxocomplexes of Group 6 Elements Mo, W, and Element 106 in Aqueous Basic Solutions. Electronic Structure and Stability.

V. Pershina and B. Fricke

Theoretical Physics Department, University of Kassel

Since a new series of the liquid chromatography experiments is to be conducted with the aim to study the behavior of element 106 in the process of extraction relative to the lighter analogs Mo and W, a theoretical investigation of the complex formation of E106 in acidic/basic solutions as well as of stability of different oxidation states is of importance.

Thus, the electronic structure of the oxyanions $[MO_4]^{2-}$, where M = Cr, Mo, W, and E106, which are basic units of many crystalline compounds (for Cr, Mo, and W) and independent units in basic solutions in the one-atom-at-a-time liquid chromatography experiments has been calculated using the Dirac-Slater Discrete Variational method. Results of the calculations are summarized in Table 1.

Table 1. Energies (negative) of molecular levels, energy gap (ΔE) and crystal-field (Δ) parameters (in eV), effective charges (Q_M) and overlap populations (OP) for $[MO_4]^{2-}$, (M = Cr, Mo, W, and E106)

Parameter	$[CrO_4]^{2-}$ 1.64 Å	$[MoO_4]^{2-}$ 1.759 Å	$[WO_4]^{2-}$ 1.786 Å	$[E106O_4]^{2-}$ 1.84 Å
E[a]	6.14	6.23	6.25	6.56
E[b]	2.77	1.98	1.53	1.72
ΔE	3.37	4.25	4.72	4.84
Δ(calc.)	1.50	1.72	1.07	0.96
Δ(exp.)[1]	1.22	1.69	1.13	-
Q_M	0.73	0.71	0.71	0.58
OP	2.10	2.28	2.81	2.84

[a] Highest occupied MO; [b] lowest unoccupied MO.

The OP data show an increase in the metal-oxygen bonding in going from the Cr to E106 complex. In aqueous solutions the $[E106O_4]^{2-}$ will be the most stable ion due to the largest hydration energy.

The transition metal complexes with the central metal atom in the maximum oxidation state is known to luminesce. To see whether the complex of E106 would have this property we have calculated energies of the charge-transfer excitations responsible for the luminescence. Obtained values are given in Table 2. From Table 2 one can see that there is an increase in $E_{\pi-d}$ of $[E106O_4]^{2-}$ indicating a strong possible luminecsence of this complex in the blue-violet area.

The calculated $E_{\pi-d}$ for the ions in the aqueous phase are also listed in Table 2. These values have been used to estimate stability of the maximum oxidation state (+6) of element 106 in aqueous solutions. The correlation between the energies of the charge-transfer transitions in the $[MO_4]^{2-}$ complexes and standard redox potentials $E^0(MO_4^{2-}/MO_4^{3-})$ gives the value of $E^0(E106O_4^{2-}/E106O_4^{3-})$ equal to -1.60 V (Fig. 1).

Table 2. Lowest energies of the charge-transfer transitions ($E_{\pi-d}$) for $[MO_4]^{2-}$, (M = Cr, Mo, W, and E106) and redox potentials $E^0(MO_4^{2-}/MO_4^{3-})$

	$[CrO_4]^{2-}$	$[MoO_4]^{2-}$	$[WO_4]^{2-}$	$[E106O_4]^{2-}$
R^a_{M-O}	1.64 Å	1.759 Å	1.786 Å	1.84 Å
$E_{\pi-d}$, eV (calc.)	3.36	4.50	5.00	5.07
$E_{\pi-d}$, eV (exp.)[2]	3.32	≃4.50	5.17	-
R^b_{M-O}[b]	1.66 Å	1.77 Å	1.79 Å	1.85 Å
$E_{\pi-d}$, eV (calc.)	3.32	4.44	4.99	5.06
$E_{\pi-d}$, eV (exp.)[3]	3.32	5.34	6.23	-
$E^0(MO_4^{2-}/MO_4^{3-})$, V	0.1	(-1.0)[c]	(-1.55)[d]	(-1.60)[d]

[a] Bond lengths in the solid state. [b] Estimated bond lengths in solutions. [c] Ref. 3. [d] Estimated value (this work).

Thus, (+6) oxidation state of E106 is only slightly more stable than (+6) oxidation state of W. This in another confirmation of a relative decrease in the stability of the maximum oxidation state in going from group 4 to group 6. Provided $[E106O_4]^{2-}$ has larger bond distances than those for which the results of the calculations are shown, it will have the stability of the (+6) oxidation state lower than that of W. An increase in the metal-oxygen bond length of 0.03 Å of the element 106 oxoanion will give the $E^0(E106O_4^{2-}/E106O_4^{3-})$ equal to -1.34 V.

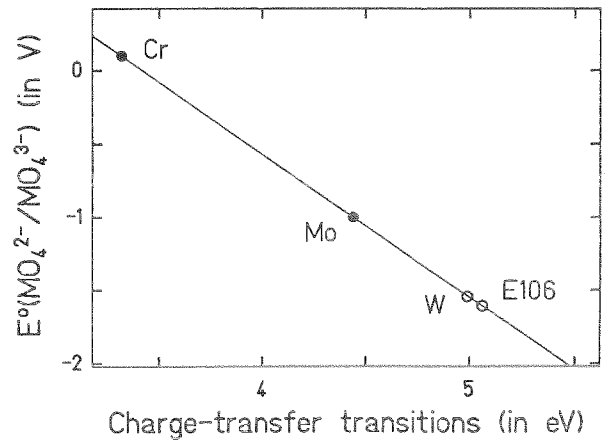

Fig. 1. Correlation between standard redox potentials $E^0(MO_4^{2-}/MO_4^{3-})$ and energies of the lowest charge-transfer transitions in the $[MO_4]^{2-}$ complexes of Cr, Mo, W, and E106.

1. A. Müller and E. Dieman, Chem. Phys. Lett., 9, 369 (1971).
2. G. Blasse and W. J. Schipper, Phys. Stat. Sol., 25, 63 (1974).
3. S. G. Bratsch, J. Phys. Chem. Ref. Data, 18, 1 (1989).